Proceedings of
10th European Conference on Turbomachinery Fluid dynamics & Thermodynamics
ETC10, April 15-19, 2013, Lappeenranta, Finland

APPLICATION OF THERMOCHROMIC LIQUID CRYSTAL MIXTURES FOR TRANSIENT HEAT TRANSFER MEASUREMENTS

C. Waidmann - R. Poser* - J. von Wolfersdorf**

* Institut of Aerospace Thermodynamics (ITLR), University of Stuttgart, 70569 Stuttgart, Germany
E-mail: christian.waidmann@itlr.uni-stuttgart.de

ABSTRACT

An approach to use mixtures of thermochromic liquid crystals (TLCs) in transient heat transfer experiments is presented. Multiple TLC indications in a single experiment increase measuring accuracy for experiments where the range of indication times would be too wide when using only a single TLC-type or by providing additional measurement information [Talib et al. (2004)]. For this study, five types of narrowband TLCs with indication temperatures between 30 °C and 50 °C have been used. TLC-mixtures and single TLCs were calibrated simultaneously and repeatedly to investigate possible aging effects. For comparison purposes a single-jet impingement plate test setup has been used. Transient experiments were then conducted for a generic turbine blade internal cooling channel configuration with a 180°-turn and ribbed walls. A technique to filter and process the signals of the green-channel and to match the intensity peaks to the respective sort of TLCs is presented in relation to Poser et al. (2009) and the results with respect to heat transfer coefficient evaluations for the cooling configuration are given. The results indicate the possibility to detect via the TLC-indications regions of unsteady heat transfer in complex flow situations

NOMENCLATURE

ρ_w	$[kg/m^3]$	Density of Perspex
Θ	$[-]$	Dimensionless temperature
$c_{p,w}$	$[J/kgK]$	Specific heat capacity of Perspex
h	$[W/m^2K]$	Heat transfer coefficient
k_w	$[W/mK]$	Thermal conductivity of Perspex
s_h	$[W/m^2K]$	Variance in heat transfer coefficient
t	$[s]$	Time
t_{Gmax}	$[s]$	TLC indication time (maximum intensity of green channel)
T_0	$[°C]$	Initial temperature
T_f	$[°C]$	Fluid temperature
T_w	$[°C]$	Wall temperature
T_{TLC}	$[°C]$	TLC indication temperature
ΔT	$[K]$	Temperature difference
(x,y)	$[-]$	Pixel position
HTC		Heat Transfer Coefficient
MIX		Mixture of Thermochromic Liquid Crystals
RTD		Resistance Temperature Device
TLC		Thermochromic Liquid Crystal

INTRODUCTION

Liquid Crystal Thermography is a widely used measuring method in heat transfer studies. Coatings of TLCs indicate the local temperature distribution of heat transfer surfaces, which can be used to determine heat transfer coefficients (HTCs) [Ekkad and Han (2000) and Ireland and Jones (2000)]. A detailed description of an advanced transient technique for turbine blade cooling circuits is given in Poser and von Wolfersdorf (2010). A fluid temperature step change induces the colorplay of the TLCs, which is captured by an RGB video camera. A temporal analysis of the video information yields the indication times of the TLCs for every pixel (e.g. maximum green intensity). Additionally, thermocouples measure the fluid temperature development and provide the internal boundary conditions for a 2D-interpolation of the fluid temperature field. Local heat transfer coefficients can then be calculated by applying the analytical solution of Fourier's equation for one-dimensional heat conduction in a semi-infinite wall with a convective boundary condition. An uncertainty analysis for this technique is given in Poser et al. (2005).

As this technique provides only one correlation between temperature and time for every pixel, it may be insufficient for complex applications; for example configurations with long cooling channels, where the fluid temperature strongly depends on the streamwise position or for applications with high local heat transfer variations. Indication times for areas with high HTCs would be very short, causing high time-uncertainties. They might even be too short to be detected due to a limitation of the camera frame rate (typically around 15 fps). The indication times for areas with low HTCs, however, would be too long and might even exceed the allowable testing time, which is limited depending on the material properties and thickness of the wall. Due to the increasing influence of lateral heat conduction over time, the measurement accuracy further decreases for long indication times, as the assumption of one-dimensional heat conduction no longer applies.

A possible solution is to divide the surface into several sections depending on their heat transfer level and to conduct several experiments with different TLCs and varying flow temperature settings. Thus, the sections can be evaluated separately by taking only those experiments into account whose indication times are in a suitable range. Another possibility is the usage of TLC-mixtures or layers of TLCs with different indication temperatures to obtain several correlations between temperature and time from a single experiment. Blair et al. (1991) used a mixture of eight different narrowband TLCs to investigate a rotating radial cooling channel configuration. Talib et al. (2004) applied a mixture of three different narrowband TLCs. They matched the obtained full intensity history of the TLC-colorplay (green signal) to a precalculated lookup table consisting of ideal intensity-histories to yield the distributions of HTCs and adiabatic wall temperatures simultaneously. In order to calculate the lookup table, an intensity vs. temperature-calibration curve had to be determined by means of a transient calibration method. Ling et al. (2004) used a similar method for film cooling applications. They calculated a lookup table containing ideal intensity histories for different combinations of HTC and η (film cooling effectiveness).

The presented method is a peak detection method. Unlike the approach of Talib et al. (2004) and Ling et al. (2004), who use the full intensity history, this method provides less (in this study five) correlations between temperature and time during the transient experiment to determine HTCs. However, this method does not require transient calibration and can apply advanced accurate peak detection and data analysis algorithms described by Poser and von Wolfersdorf (2010).

TEST FACILITIES AND PROCEDURE

In this study five types of narrowband encapsulated liquid crystals with varying indication temperatures have been examined, as given in Table . TLCs do not emit light, they selectively reflect light of a specific wavelength due to thin film effects. To get the full spectrum of the TLC colorplay,

[1]LCR Hallcrest Ltd, UK

designation	indication temp. (green start)	type[1]	bandwidth
TLC30	30 °C	SPN/G30C1W	1 K
TLC35	35 °C	SPN/G35C1W	1 K
TLC40	40 °C	SPN/G40C1W	1 K
TLC45	45 °C	SPN/G45C1W	1 K
TLC50	50 °C	SPN/G50C1W	1 K

Table 1: **Thermocromic liquid crystals**

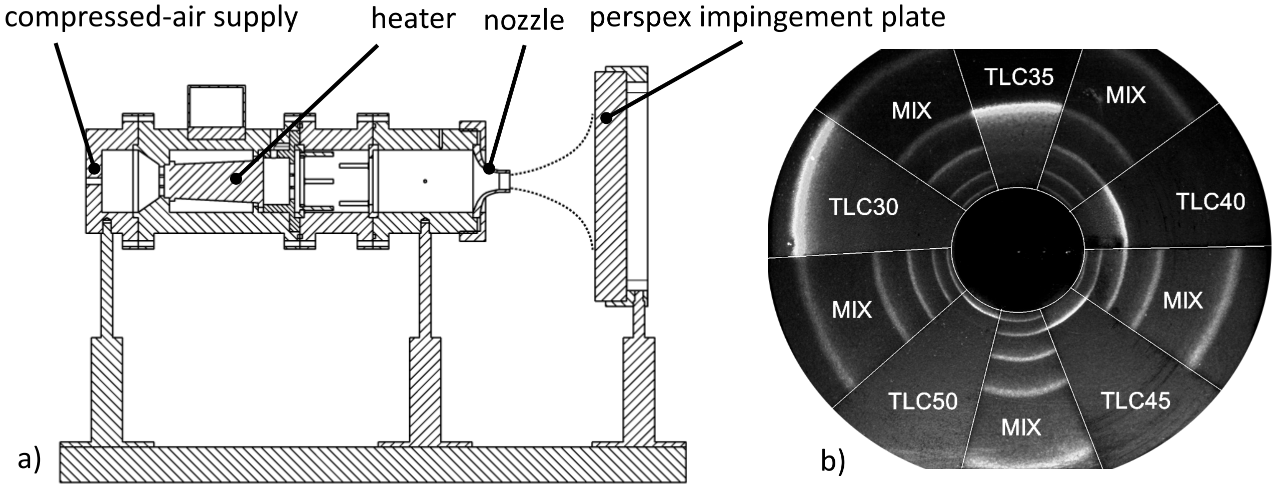

Figure 1: **a) Single jet impingement test facility; b) Comparison of TLC mixture and single TLCs**

the illumination must have a broad spectrum and has to contain all required wavelengths. For all experiments OSRAM De Luxe Warm White (930) fluorescent lamps with a color temperature of 3000 K were used for illumination.

Single Jet Impingement Facility

First experiments with TLC-mixtures were conducted on a single-jet impingement test facility, as shown in Figure 1. Five TLCs were premixed with an equal mass ratio of 1:1:1:1:1 (MIX) and applied to the impingement Perspex plate using an airbrush system. The TLCs were then covered with a black backing paint. A mixture was preferred as opposed to applying the different TLC types in layers to achieve a single, homogeneous layer. Pretests have shown that the application of layers can lead to unacceptable high layer thicknesses. The heated air jet impinges on the coated plate side and the colorplay of the TLCs was captured through the perspex plate by a digital color video camera (Dalsa DS-22-02M30).

The facility can provide an air-jet with varying temperatures and exit velocities which mixes with the surrounding colder ambient air thus creating a temperature distribution on the nearly adiabatic impingement plate in a thermal steady state situation. The gained temperature field on the plate (the adiabatic wall temperature distribution) should be rotationally symmetric with a hot center and radially decreasing temperatures. Thus, circular-shaped isotherms are expected. The plate was divided into several sectors on which the MIX and the five single TLCs were alternatingly applied with the same approach to achieve comparable layer thicknesses, as shown in Figure 1 b). The image was taken after the plate has reached steady-state. The green indication lines show a smooth transition from a sector with a mixture to a sector with a single TLC. Thus, there is no significant shift in the indication temperature between a mixture and a single TLC. Whereas this basic characteristic (i.e. temperature

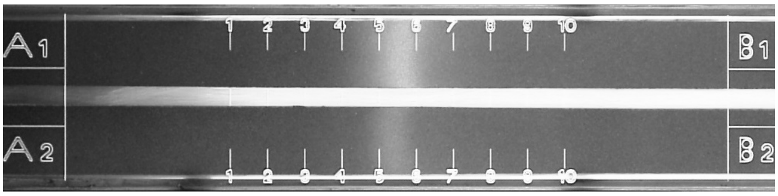

Figure 2: **Copper calibration plate, TLC30 (upper side) MIX (lower side)**

	$T_{singleTLC}$ [°C]	T_{MIX} [°C]	deviation [K]
TLC30	29.55	30.23	0.68
TLC35	35.08	35.15	0.07
TLC40	39.47	39.19	0.28
TLC45	44.36	44.35	0.01
TLC50	49.26	49.22	0.04

Table 2: **TLC calibration, comparison single TLC vs. MIX**

dependency) remains, it can be clearly seen that the intensity of the reflected light is significantly lower for the MIX compared to a single TLC. This can be explained by the lower particle (capsule) density per area, for a TLC type in the MIX compared to the respective single TLC. Intensity can drop down to 50% of the single TLC intensity. Therefore, an intensity method rather than a hue method is applied for data analysis. Intensity methods are much more sensitive for weak signals [see Poser et al. (2007)] and become crucial for TLC mixtures. An intensity-independent evaluation method is achieved by adaptive normalization of the intensity signal.

Calibration Facility

Calibration is needed to determine the indication temperature, i.e., the temperature at which the intensity of the green color channel reaches its maximum. The calibration facility consists mainly of a rectangular copper plate, suitable to provide a linear temperature gradient on its surface. This is achieved by cooling one side while heating the other side constantly and insulating the side walls. 10 thermocouples (Type T) are placed equidistantly along the centerline just below the surface. They were calibrated using calibrated high precision mercury thermometers with a reading accuracy of 0.1 K. For cold junction compensation the thermocouple connections to the temperature scanner are located inside an isothermal aluminum block, whose temperature is measured by an RTD (type Pt100). A linear regression line was fitted to the thermocouple measurements along the copper plate. Thereby the deviation of the single thermocouple readings from the fitted line was less than 0.05 K. In Figure 2, the copper plate is coated with TLC30 (upper side) and the MIX (lower side). The five indications of the MIX cannot be generated on the plate simultaneously as the required temperature gradient would be too steep. Therefore, each indication is calibrated separately by setting the plate temperatures, so that the maximum intensity of the respective green indication appears approximately in the middle of the plate. The plate has to reach steady-state before each calibration, which is verified by monitoring the thermocouples. The calibration for the entire set of five indications takes about five days including heating and cooling phases for confirmation. Table contains the calibrated indication temperatures for the single TLC and the MIX. The measurement uncertainty for this stationary TLC calibration was evaluated to less than 0.2 K. The measured indication temperatures have a maximum deviation between the MIX and the single TLC of 0.68 K. Thus, the results of a single TLC calibration cannot be applied directly to experiments with TLC mixtures. Mixtures must always be calibrated separately. Calibration was repeated after 3 weeks and again after 5 weeks to examine possible aging effects. The

	1. week T_{MIX} [°C]	4. week T_{MIX} [°C]	6. week T_{MIX} [°C]	max. deviation [K]
TLC30	30.18	30.23	30.14	0.09
TLC35	35.06	35.15	35.10	0.09
TLC40	39.00	39.19	39.09	0.19
TLC45	44.26	44.35	44.39	0.13
TLC50	49.00	49.22	49.17	0.22

Table 3: **Repeated calibration**

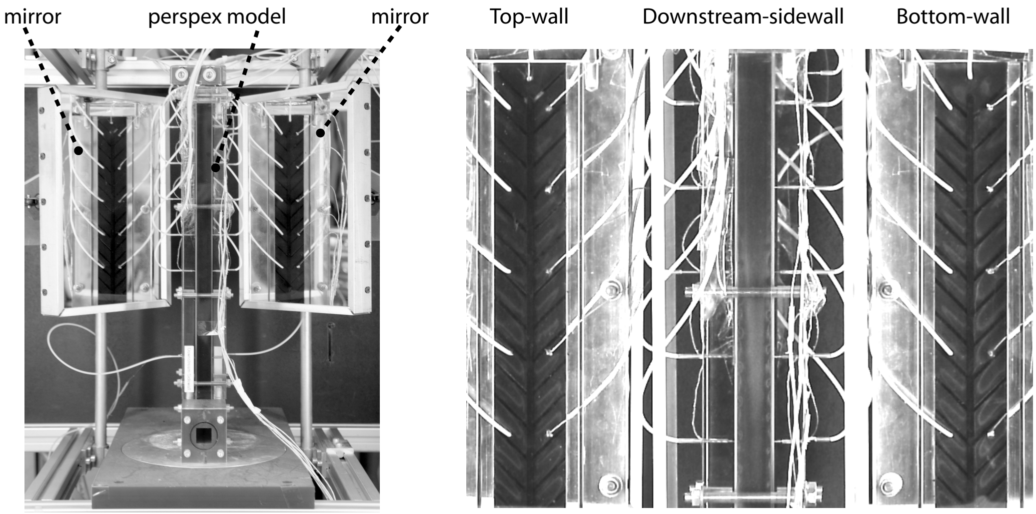

Figure 3: **Perspex model on transient heat transfer test facility**

results are given in Table . No significant shift of the indication temperature due to aging effects can be detected. The maximum deviation of 0.22 K for TLC50 is comparable to the measurement uncertainty.

Transient Heat Transfer Test Facility

A generic model of a turbine blade cooling channel configuration was tested using a transient heat transfer test facility. Figure 3 shows the perspex model mounted on the test facility. The model contains a cooling channel with a rectangular cross-section, 180°-turn and ribbed top- and bottom-walls. The inner walls are coated with the MIX and black paint. The test facility provides a fluid temperature step change by suddenly leading heated air through the model. While the channel wall temperature rises, a color video camera (Sony DFW-X710) with a resolution of 1024 x 768 pixels captures the TLC-colorplay through the perspex at a frame rate of 15 fps. The temperature step is set appropriately so that a surface temperature above 50 °C is reached at each position for a full transition of all five TLC types. Typical test durations are less than 60 s. Using mirrors, three heat transfer surfaces can be captured simultaneously with a single camera. In Figure 4, the history of an exemplary pixel line of the bottom wall is depicted. The normalized video (as described in the following chapter) was used to create the image. The pixel line was extracted from every video frame and concatenated to a 2D-representation of the pixel line history. It can be seen, that the five indications occur at different points of time, depending on the pixel position.

SIGNAL PROCESSING AND PEAK DETECTION

Figure 5a shows the exemplary intensity history for the RGB-channels of a single pixel. Prior to peak detection, the signal has to be preprocessed [Poser et al. (2009)]. Each color channel has an

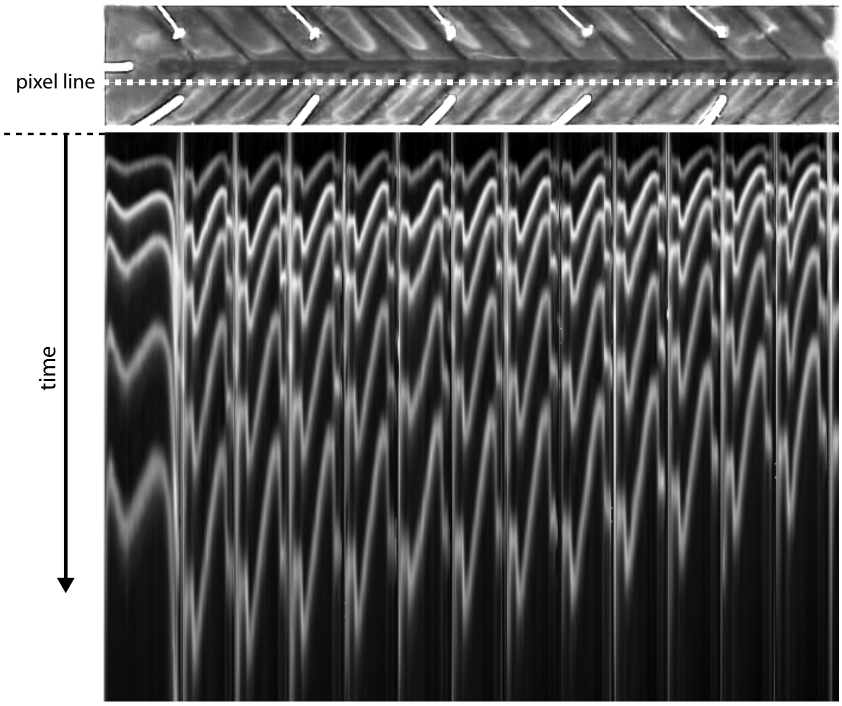

Figure 4: **Pixel line history (normalized video)**

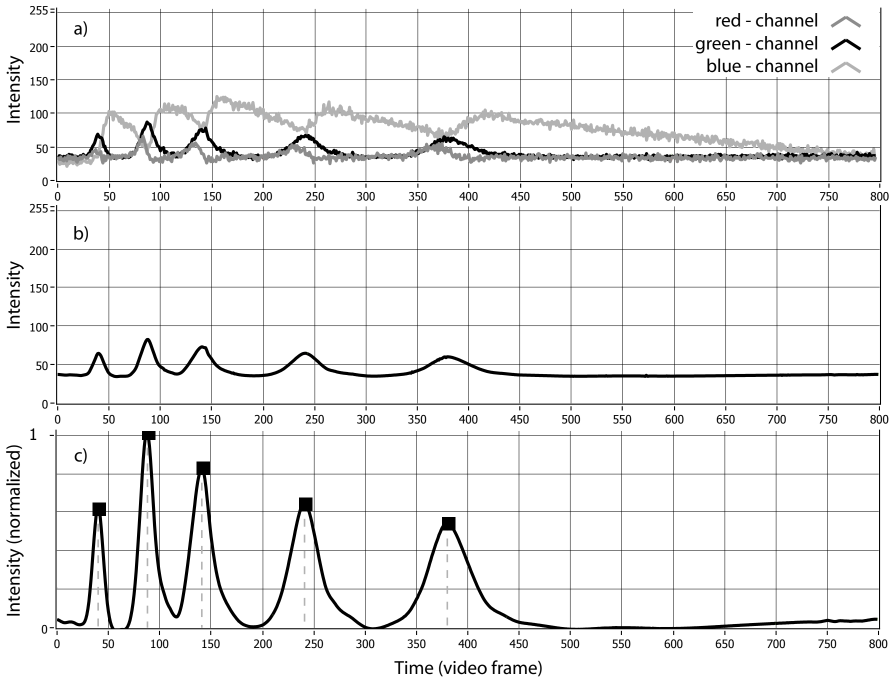

Figure 5: **Intensity history for one pixel a) Original RGB; b) Wavelet-filtered green-signal; c) Normalized green-signal**

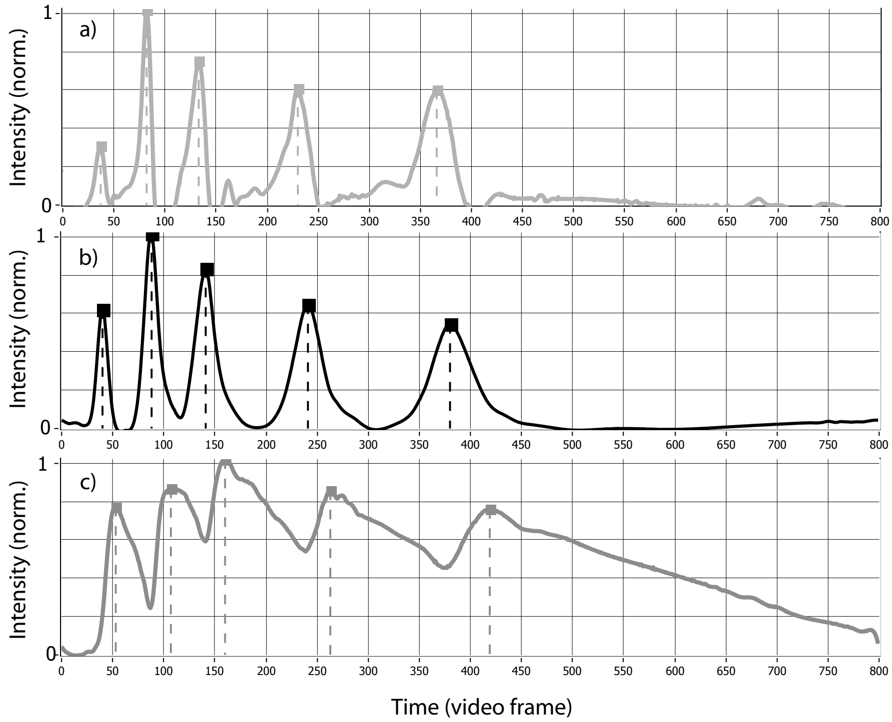

Figure 6: **Peak detection for wavelet-filtered and normalized intensity history a) red-channel; b) green-channel; c) blue-channel**

8 bit integer bandwidth which corresponds to a gray level range from 0 to 255. A discrete wavelet filter (undecimated discrete FBI wavelet) is used for noise-filtering. Figure 5b shows the noise-filtered green signal. Unlike other filtering techniques like moving-average, wavelet-filtering does not shift the positions of peaks in time. Subsequently, the signal is normalized by setting the global maximum to 1 and the base level of the signal to 0. Uniform illumination of complex geometries and curved surfaces is difficult and cannot be realized for every experiment. However, by adaptive normalization the influence of insufficient illumination can be minimized. Figure 5c shows the normalized green-signal. Here, the peak of the second indication has the highest intensity. Wavelet-filtering and normalization is done separately for each color-channel of every pixel. Figure 6 shows the preprocessed RGB-signals for one exemplary pixel. Using these preprocessed RGB-signals, a normalized video can be rendered showing virtual hue values, as the resulting colorplay does not represent the original visual spectrum. This video was used to create the pixel line history in Figure 4. For peak detection, the routine *WA Multiscale Peak Detection VI* implemented in the *Advanced Signal Processing Toolkit* by *LabVIEW* [2] is used. In order to detect only the peaks that correspond to the respective indication, some input-values are required. The threshold-value assures that peaks with an amplitude below a specific value are ignored. The threshold can be set in a range from 0 (no threshold) to 1 (only the highest peak is detected). By setting the width-value (in number of samples or in this case video frames) only peaks of a minimum width are taken into account. Figure 7 shows a contour-plot of the bottom-wall representing the number of detected peaks in the green-signal. A pixel with five detected peaks is grey. A lower number of peaks is illustrated light grey and a higher number of peaks is illustrated black. As there is no valid TLC indication on the ribs and on the pressure measurement tubes (see Figure 3), these regions are blanked. It can be seen that the peak detection works well for almost all areas. In some areas less than five peaks are detected, especially in the corners between the ribs and the web. Areas with more than five peaks are observed. In the vicinity downstream of the ribs, where the flow reattaches, thin streaks appear

[2]**Lab**oratory **V**irtual **I**nstrumentation **E**ngineering **W**orkbench™ by National Instruments

Figure 7: **Number of detected green signal-peaks (bottom-wall; threshold: 0.20; width: 16)**

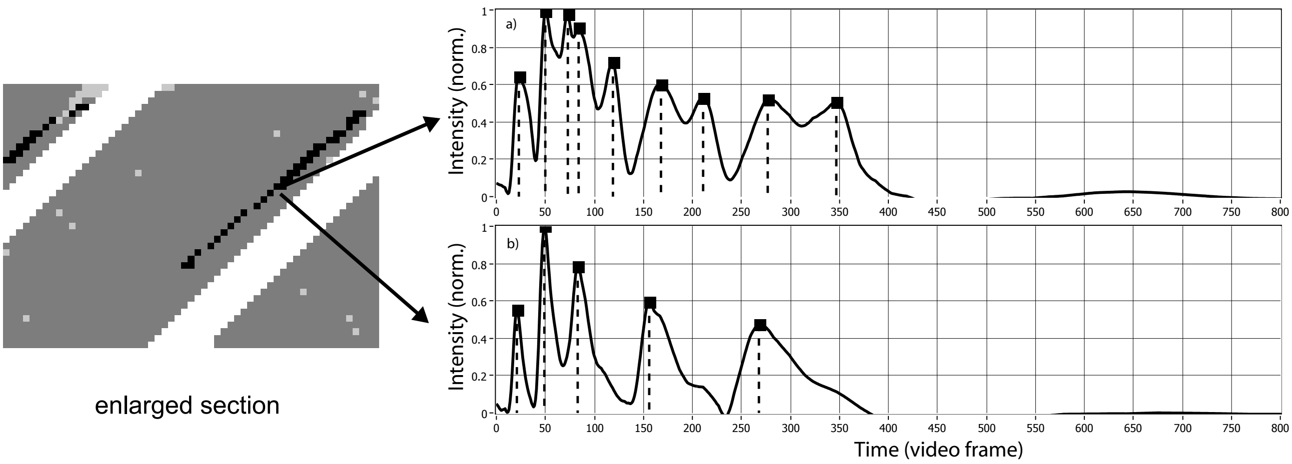

Figure 8: **Peak detection of green signal a) inside streak b) outside streak**

where peak detection fails. These areas have to be examined separately. Figure 8 shows an enlarged section of the area around such a streak and a comparison of the preprocessed signals of a pixel inside the streak and a neighboring pixel outside of the streak. Due to increased turbulence in the reattaching flow and flow recirculation regions, some TLC types indicate more than once (suggesting unsteady flow phenomena) causing a flicker in the signal of the pixels inside the streak. For the exemplary signal shown in Figure 8 a) nine peaks are detected. However, a correct assignment of the peaks to the respective indication can not be guaranteed.

HEAT TRANSFER EVALUATION

Figure 9 show the contour plots of the indication times for the five different TLCs, exemplary for the bottom-wall. Areas that are blocked by thermocouples or pressure tubes and areas with more or less than five detected peaks are interpolated. These indication time arrays can be directly imported into existing data analysis processes to evaluate the local heat transfer coefficients as described by Poser and von Wolfersdorf (2010). In addition to the indication times, the local fluid temperature history at each pixel position (x,y) is required for the evaluation. Several thermocouples along the centerline of the channel provide the data for a bilinear interpolation of the fluid temperature field $T_f(x,y,t)$ for each time step. The local heat transfer coefficients h are obtained by iteratively solving the following equation

$$T_w - T_0 = \sum_{j=1}^{N} \left[1 - \exp\left(\frac{h^2(t_{Gmax} - \tau_j)}{\rho_w \, c_{p,w} \, k_w} \right) \operatorname{erfc}\left(\frac{h\sqrt{t_{Gmax} - \tau_j}}{\sqrt{\rho_w \, c_{p,w} \, k_w}} \right) \right] \cdot \Delta T_{f(j,j-1)} \qquad (1)$$

which represents the analytical solution of Fourier's one-dimensional heat conduction equation for a semi-infinite wall and a convective boundary condition, whereby the real fluid temperature history is approximated by a series of small discrete temperature steps $\Delta T_{f(j,j-1)}$ using the Duhamel super-

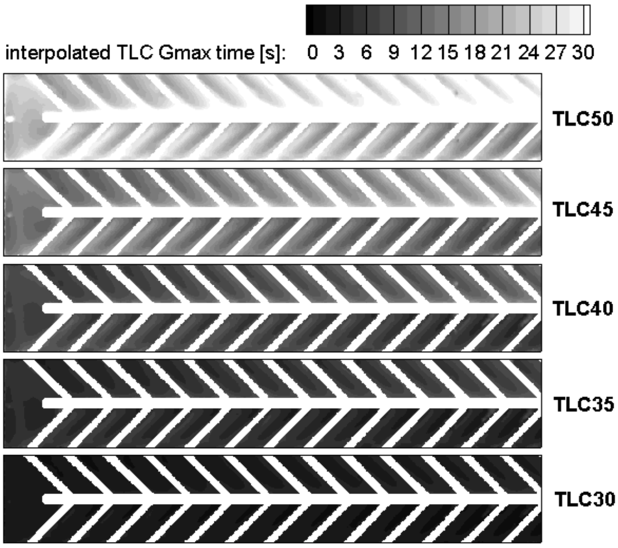

Figure 9: **Interpolated indication time (t_{Gmax})**

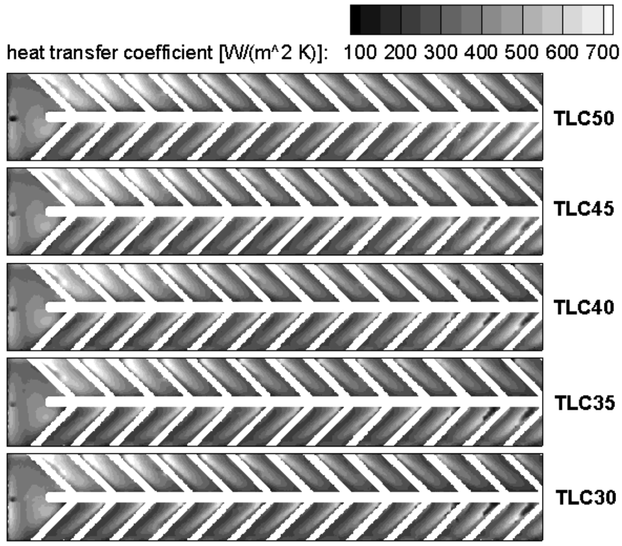

Figure 10: **Local HTC distribution**

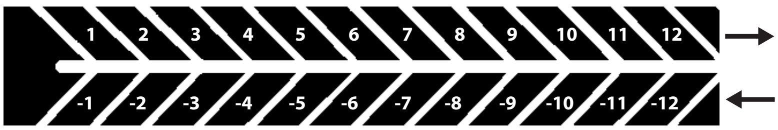

Figure 11: **Segment numbering**

position principle. In this equation $T_w = T_{TLC}$ is the wall temperature at the time of indication, T_0 is the initial model temperature and ρ_w, $c_{p,w}$, and k_w are the material properties of Perspex. Figure 10 shows the results of the heat transfer evaluation in the form of the local HTC distribution. These were obtained by evaluating each indication time array separately. For easier comparison, the local data were reduced to segment averaged values by area averaging the HTC-values of a rib-segment (i.e. sector between two ribs). Figure 11 depicts the numbering of the segments. The result is given in Figure 12. In Figure 13 the averaged HTC-values are normalized with the values of TLC50. The bend region was left out for this comparison.

The indication times are in a range of 0 to 5 seconds for TLC30 and in a range of 2 to 10 seconds for TLC35. For our experimental setup typical indication times should be in a range of 3 to 80 seconds. So this experiment was very fast for the first two TLC types. The indication times for TLC50 are in a

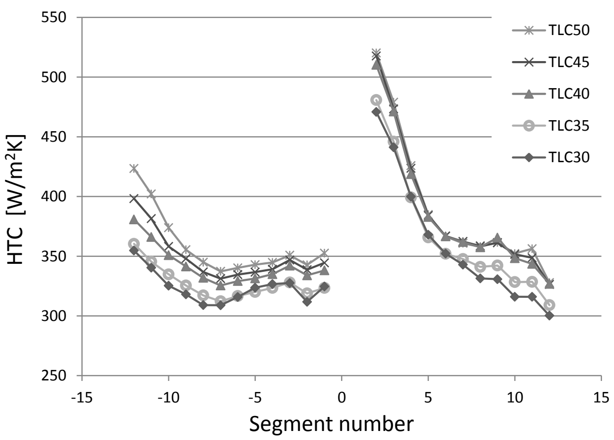

Figure 12: **Segment averaged HTC**

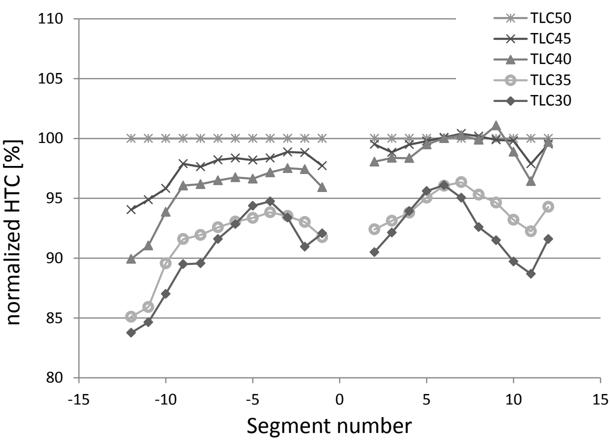

Figure 13: **Normalized HTC w.r.t. TLC50**

symbol	value	variance	unit	meaning
ρ_w	1190	10	$[^{kg}/_{m^3}]$	Density of Perspex at 20 °C
$c_{p,w}$	1470	10	$[^{J}/_{kgK}]$	Specific heat capacity of Perspex
k_w	0.19	0.01	$[^{W}/_{mK}]$	Thermal conductivity of Perspex at 20 °C
T_0	varies	0.2	$[K]$	Initial temperature
T_f	varies	0.2	$[K]$	Fluid temperature
T_{TLC}	varies	0.2	$[K]$	Calibrated TLC indication temperature
t_{Gmax}	varies	0.2	$[s]$	Detection time

Table 4: **Parameter of uncertainty analysis**

range of 15 to 45 seconds giving a good experimental range for this TLC type. The largest differences between the different TLC types occur in the inlet region. Here the indication times of TLC30 are below 2 seconds, which results in high time uncertainties. Therefore, here the results of the TLCs with the later indications (TLC40, TLC45 and TLC50) are more trustworthy. In the outlet channel we have a good agreement for TLC40, TLC45 and TLC50. The values of TLC30 and TLC35 are lower. In the inlet channel the values of TLC40, TLC45 and TLC50 have a significant deviation. The values of TLC40 are up to 10% below the values of TLC50 for the first three segments (-12, -11 and -10). Further downstream the deviations from TLC50 are below 4% for both TLC40 and TLC45.

Uncertainty analysis

The uncertainty of the evaluated HTC is dependent on uncertainties of temperature measurements, time measurements, the uncertainties of the material properties of Perspex, as well as the value of the HTC itself. Table 4 contains the influential parameters and their uncertainties. For the following considerations the uncertainties of the material properties of Perspex are not taken into account. Their influence on the uncertainty of the overall result is typically in the order of 5%. For an analysis of the temperature uncertainties the dimensionless temperature ratio Θ has to be determined.

$$\Theta = \frac{T_w - T_0}{T_f - T_0} \tag{2}$$

Due to the nature of the transient experiment the fluid temperature and the respective temperature ratio is not constant during the experiment. However, to state characteristic temperature ratios Θ for each TLC type, constant equivalent fluid temperatures $T_{f,equival}$ can be derived from the fluid temperature history. They represent a hypothetical ideal fluid temperature step that would result in the same indication time as the real fluid temperature history. Using the Gaussian error propagation principle the variance of Θ can be derived from the temperature values and their uncertainties as given in Table 4. As presented by Poser et al. (2005) additionally the time uncertainties need to be taken into account and overall uncertainty analysis depends strongly on the specific experimental parameters. Figure 14 shows the relative uncertainty of HTC for the different TLC types depending on the temperature ratio Θ considering temperature and time uncertainties and HTC level. The presented uncertainties were evaluated numerically using Mathematica®assuming a position at the channel inlet, a HTC of $h = 350\,^{W}/_{m^2K}$ and a restriction of the test duration to $t_{max} = 90\,s$. We can see that for this experiment the uncertainty levels decrease with increasing TLC indication temperatures resulting in the lowest uncertainty level for TLC50.

SUMMARY

A mixture of five TLCs was examined and the possibility of its usage in transient heat transfer experiments has been shown. The stability of the mixture has been approved by repeated calibration. A way of signal preprocessing including waveletfiltering and adaptive normalization was demonstrated

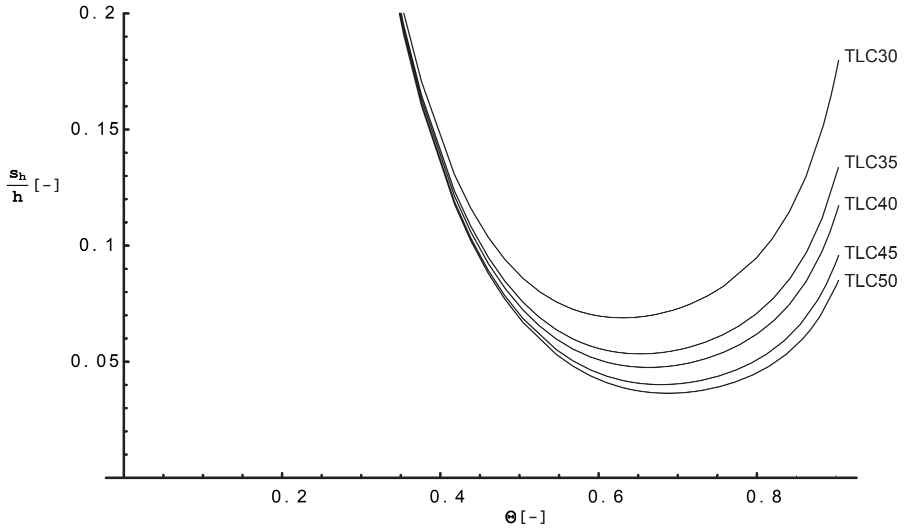

Figure 14: **Relative uncertainty of HTC for variation in temperature ratio**

on an exemplary RGB-signal captured in a transient experiment. A wavelet based peak detection technique was applied to obtain arrays containing the several TLC indication times. For most areas the detected peaks can be assigned to a respective TLC indication. However, areas of unsteady flow phenomena were identified, where more than the expected peaks are detected due to multiple indication of single TLC types in the mixture. These areas could not be evaluated and had to be interpolated for further heat transfer evaluation. The results show some deviations for the different TLC types, especially in the inlet region of the test channel. Therefore, experiments with varying temperature levels and therewith varying indication times are suggested to identify possible influences of the experiment duration on the heat transfer results. Further, the sensitivity of the results on the measured flow temperatures might be assessed using regression analysis of the data from all TLC types as used by Talib et al. (2004) to address additional uncertainties due to e.g. coating thickness.

ACKNOWLEDGMENTS

Experiments and calibration were conducted with the support of students. The work of U. Kiesewetter, S. Maier and Y. Schumann is kindly acknowledged.

References

M. F. Blair, J. H. Wagner, and G. D. Steuber. New applications of liquid–crystal thermography in rotating turbomachinery heat transfer research. *ASME, International Gas Turbine and Aeroengine Congress and Exposition, 36th, Orlando, FL, June 3-6, 1991. 11 p.*, 1991.

S. V. Ekkad and J. C. Han. A transient liquid crystal thermography technique for gas turbine heat transfer measurements. *Measurement Science and Technology*, 11(7):957–968, 2000.

P. T. Ireland and T. V. Jones. Liquid crystal measurements of heat transfer and surface shear stress. *Measurement Science and Technology*, 11(7):969–986, 2000.

J. P. C. W. Ling, P. T. Ireland, and L. Turner. A Technique for Processing Transient Heat Transfer, Liquid Crystal Experiments in the Presence of Lateral Conduction. *Journal of Turbomachinery*, 126 (2):247, 2004.

R. Poser and J. von Wolfersdorf. Transient liquid crystal thermography in complex internal cooling systems. *VKI Lecture Series - Internal Cooling in Turbomachinery, von Karman Institute for Fluid Dynamics*, (VKI LS 2010-05), 2010.

R. Poser, J. von Wolfersdorf, and K. Semmler. Transient Heat Transfer Experiments in Complex Passages: HT2005-72260. *Proceedings of HT2005 ASME Summer Heat Transfer Conference, July 17-22, 2005, San Francisco, California, USA*, 2005.

R. Poser, J. von Wolfersdorf, and E. Lutum. Advanced evaluation of transient heat transfer experiments using thermochromic liquid crystals. *Proceedings of the Institution of Mechanical Engineers, Part A: Journal of Power and Energy*, 221(6):793–801, 2007.

R. Poser, J. R. Ferguson, and J. von Wolfersdorf. Temporal Signal Preprocessing and Evaluation of Thermochromic Liquid Crystal Indications in Transient Heat Transfer Experiments. *8th European Conference on Turbomachinery Fluid Dynamics and Thermodynamics*, pages 785–795, 2009.

A. R. A. Talib, A. J. Neely, P. T. Ireland, and A. J. Mullender. A Novel Liquid Crystal Image Processing Technique Using Multiple Gas Temperature Steps to Determine Heat Transfer Coefficient Distribution and Adiabatic Wall Temperature. *Journal of Turbomachinery*, 126(4):587–596, 2004.